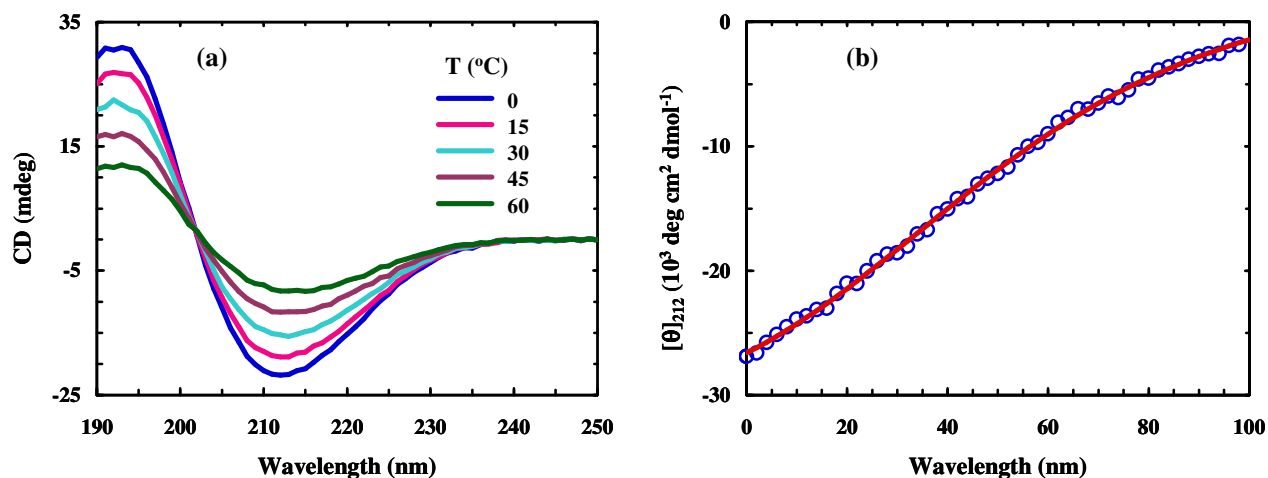


## Infrared Signature and Folding Dynamics of a Helical $\beta$ -Peptide

Geronda Montalvo<sup>&</sup>, Matthias M. Waegle<sup>#</sup>, Scott Shandler<sup>&</sup>, Feng Gai<sup>#,\*</sup> and William F. DeGrado<sup>#,&,\*</sup>

<sup>#</sup>Department of Chemistry and <sup>&</sup>Department of Biochemistry & Biophysics, University of Pennsylvania, Philadelphia, PA 19104



**Figure S1.** (a) CD spectra of the  $\beta$ -peptide collected at different temperatures, as indicated. (b) Ellipticity (open cycle) of the  $\beta$ -peptide at 212 nm as a function of temperature. The red line represents the best fit of these data to a two-state model wherein the folded and unfolded CD baselines were assumed to be independent of temperature. The folding thermodynamic parameters recovered from the fit are:  $\Delta H = -7.1$  kcal/mol,  $\Delta S = -22.4$  cal  $\text{K}^{-1}$  mol $^{-1}$ .

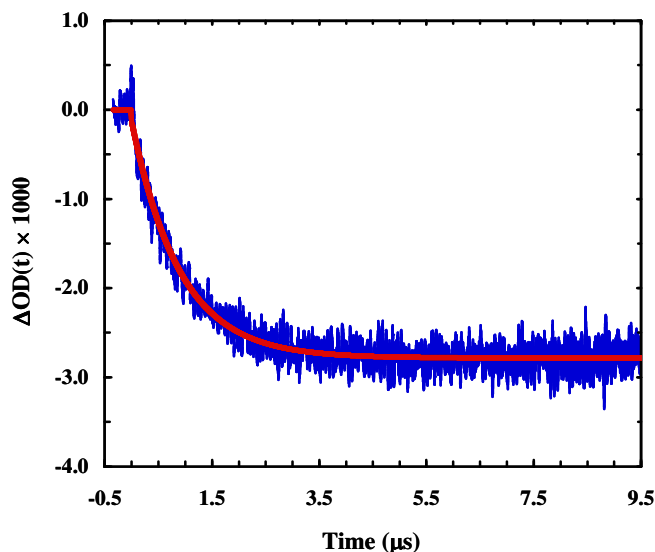


**Figure S2.** A representative relaxation kinetic trace (blue) in response to a  $T$ -jump from 9.2 to 16.5  $^{\circ}\text{C}$ . The red line represents the best fit of the data to a single-exponential function ( $\tau = 0.9$   $\mu\text{s}$ ) convoluted with the instrument response function. The probing frequency was 1614  $\text{cm}^{-1}$ .

**Peptide Synthesis:** The  $\beta$ -peptide was synthesized on a CEM Discover microwave synthesizer using  $\alpha$ -D-Asp-Wang resin (NovaBiochem 0.75 mmol/g substitution) for support of  $\beta^3$ -amino acids (PepTech Corporation). The resin was first swelled in 100% dimethylformamide (DMF, Fisher Scientific) for about one hour, which was followed by deprotection using 30% piperidine first and then 2% piperidine (Sigma-Aldrich), 2% 1,8-Diazabicyclo[5.4.0]undec-7-ene (DBU, Aldrich), 96% DMF. The deprotection process was carried out in the microwave at 70 °C and 30 W for 6 minutes. The  $\beta^3$ -amino acids were then coupled to the resin using 3 equivalents of amino acid, 2.8 equivalents of 2-(1H-7-Azabenzotriazol-1-yl)-1,1,3,3-tetramethyluronium hexafluorophosphate Methanaminium (HATU, GL Biosciences) activator, and 3 equivalents of diisopropylethylamine (DIEA, CHEM-IMPEX International) for 10 minutes in the microwave. The resin was washed three times each with DMF, dichloromethane (DCM, Fisher Scientific), and DMF again. This step was followed by deprotection (as described above); this and the subsequent steps were repeated for the remaining residues in the peptide sequence. Following deprotection of the final residue the  $\beta$ -peptide was cleaved from the resin using a cocktail of 2:2:2:94 H<sub>2</sub>O:TIS (triisopropyl silane):Anisole:TFA (trifluoroacetic acid) (all obtained from Sigma-Aldrich) for 2 hours at room temperature. The peptide was collected separately from the resin and was precipitated using a cold ethyl ether/hexanes mixture (50/50, v/v). The precipitate was dried on the lyophilizer and was then purified using reversed-phase high performance liquid chromatography (HPLC, Varian ProStar) on a Vydac peptide C4 prep column. The mass of the  $\beta$ -peptide product was verified by matrix-assisted laser desorption/ionization mass spectrometry (MALDI-MS, Voyager-DE RP). All peptide samples were prepared by directly dissolving lyophilized peptide solids into 20 mM phosphate buffer (pH 7). For CD measurement, the peptide concentration, which was determined optically using Tyr absorbance, was in the range of 30-90  $\mu$ M, whereas for IR measurements, the peptide concentration was approximately 5 mM.

**CD and FTIR Measurements:** All CD data were collected on a Jasco CD spectropolarimeter (J-810) using a 1 mm sample cuvet. FTIR spectra of the  $\beta$ -peptide in D<sub>2</sub>O phosphate buffer (20 mM, pH 7) were collected on a Nicolet Magna-IR 860 spectrometer using 1 cm<sup>-1</sup> resolution. The details of the setup were given in reference 1.

**Global Fitting of the FTIR Spectra:** The temperature-dependent FTIR spectra in the amide I' region, i.e.,  $S(T, \nu)$ , were modeled globally with six Gaussians whose positions and widths were allowed to vary with respect to temperature:

$$S(T, \nu) = \sum_1^6 G_i(A_i, \nu_i, \Delta \nu_i) + LB(T) \quad (1)$$

where  $LB(T)$  is a linear baseline that was introduced to account for the small background presented in the data, and  $G_i(A_i, \nu_i, \Delta \nu_i)$  is defined as

$$G_i(A_i, \nu_i, \Delta \nu_i) = A_i \exp \left( - \ln(2) \left( \frac{\nu - \nu_i(T)}{\Delta \nu_i(T)} \right)^2 \right) \quad (2)$$

Here,  $A_i$  is the band amplitude, which was treated as a local variable in the fit.  $\nu_i(T)$  and  $\Delta \nu_i(T)$  are band position and bandwidth (full width at half maximum), respectively, and were assumed to be linearly dependent on temperature,

$$\nu_i(T) = \nu_i(0) + \rho_i(T - T_0) \quad (3)$$

$$\Delta \nu_i(T) = \Delta \nu_i(0) + \lambda_i(T - T_0) \quad (4)$$

Here,  $T_0$  is a reference temperature and was set as the lowest temperature used in the experiment;  $\nu_i(0)$ ,  $\Delta \nu_i(0)$ ,  $\rho_i$ , and  $\lambda_i$  are constants and were treated as global variables in the fitting.

**T-jump Setup:** The T-jump setup was the same as described in reference 1, except that a CW QC laser (Daylight Solutions, CA) was used as the infrared probe in the current study.

**Molecular Dynamics Simulation:** An ideal 14-helix was generated using in house code based on the sequence of the  $\beta$ -peptide. Briefly, using an interpretive bonding algorithm, a 15 residue  $\beta$ -amino acid (C-terminal  $\alpha$ -amino acid) scaffold was analyzed for proper atomic connectivity and the 14-helix backbone dihedral angles were appropriately set ( $\phi = 120$ ,  $\psi = 55$ ,  $\theta = -140$ ,  $\omega = 170$ ). Next, the amino acid sequence was loaded onto the helical scaffold, using the most energetically favorable rotameric state for each amino acid in the C<sup>3</sup> position.<sup>2</sup> All sidechains were modeled using the L-stereochemistry except the C-terminal  $\alpha$ -Asp, which was modeled using D-stereochemistry. This C-terminal capping motif has been shown beneficial in helix nucleation.<sup>3</sup> The resulting model was checked for clashes and minimized using the XPLOR package.<sup>4</sup> After a brief energy minimization (200 steps) in vacuum, the 14-helix was then solvated in a box containing 4265 TIP3P water molecules. As the  $\beta$ -peptide has a net charge of -1 at pH 7.0, a sodium ion was also added to neutralize the system. While harmonically restraining all peptide atoms with a force constant of 10 kcal/mol/Å<sup>2</sup>, the energy of the entire system was minimized for 2000 steps and simulated at 1 atm and 300 K for 200 ps to allow the water molecules to populate the hydration sites. After removal of the harmonic restraints, an energy minimization was again performed for 4000 steps and then the system was allowed to equilibrate for another 4 ns. Following equilibration, a 1 ns production run was carried out in the NPT ensemble under identical conditions. While the Berendsen barostat was used to relax the system to equilibrium, pressure was maintained at 1 atm using the Nosé-Hoover Langevin piston method for the production run. Temperature was controlled by Langevin dynamics and periodic boundary conditions were used to reduce edge effects. The SHAKE algorithm was employed to constrain all bonds involving hydrogen. A cut-off of 12 Å was used for non-bonded interactions, which were switched to zero between 10 and 12 Å. Full electrostatics were calculated every second step using the particle-mesh Ewald (PME) method. A 2 fs time step was used to integrate the equations of motion and coordinates were saved every 0.1 ps for analysis. The  $\beta$ -peptide backbone dihedral parameters were estimated from standard CHARMM force field parameters and chosen in such a way that the dihedral angles of the ideal helical structure correspond to the energy minima. Within the 1 ns production run, the average RMSD of the heavy backbone atoms from the *in vacuo* optimized starting 14-helix structure was 0.94 Å. All simulations were carried out in the NMAD package,<sup>5</sup> and VMD<sup>6</sup> was used to analyze coordinates.

**Amide I band Calculation:** The amide I band of the 14-helix was calculated based on the local amide I Hamiltonian.<sup>7-12</sup> In this model, one oscillator is assigned to each peptide group, resulting in a  $n \times n$  Hamiltonian matrix for a system containing  $n$  peptide bonds. Upon diagonalization of the local amide I Hamiltonian, the  $n$  frequencies (eigenvalues) and the corresponding vibrational modes  $\mathbf{T}_n$  (eigenvectors) of the exciton system are obtained. The product of an eigenvector  $\mathbf{T}_n$  with the  $n \times 3$  transition dipole matrix  $\mathbf{d}$ , which contains the Cartesian components of the transition dipoles for the  $n$

peptide groups, gives the transition dipole for the corresponding frequency. The Hamiltonian was constructed by assigning a vibrational frequency of  $1650\text{ cm}^{-1}$  to the diagonal elements<sup>8</sup> and calculating the off-diagonal elements based on the transition dipole coupling model:<sup>7-12</sup>

$$V_{ij} = A \frac{\hat{\mu}_i \cdot \hat{\mu}_j - 3(\hat{\mu}_i \cdot \hat{n}_{ij})(\hat{\mu}_j \cdot \hat{n}_{ij})}{r_{ij}^3}$$

where  $A = 580\text{ cm}^{-1}\text{\AA}^3$ ,  $\hat{\mu}_i$  is the unit transition dipole of the  $i$ th amide I mode,  $\hat{n}_{ij}$  is the unit vector connecting the dipoles, and  $r_{ij}$  is the distance between the dipoles. The transition dipole was assumed to be located  $0.868\text{ \AA}$  away from the carbon along the carbonyl bond axis with an orientation of  $20^\circ$  off the C=O axis towards the nitrogen.<sup>7,8</sup>

The calculation was carried out on every structure of the production run, which produced a total of 10,000 structures. The resulting 140,000 frequencies and their associated transition dipoles were then summed on a grid with a spacing of  $1\text{ cm}^{-1}$ , yielding the stick spectrum shown in Figure 3.

## Reference

1. Huang, C. Y.; Getahun, Z.; Zhu, Y.; Klemke, J. W.; DeGrado, W. F.; Gai, F. *Proc. Natl. Acad. Sci. U.S.A.* **2002**, *99*, 2788-2793.
2. Shandler, S.; Shapovalov, M.; Dunbrack, Jr, R.; DeGrado, W. F. *J. Am. Chem. Soc.* **2010** (in press).
3. Goodman, J. L.; Petersson, E. J.; Daniels, D. S.; Qiu, J. X.; Schepartz, A. *J. Am. Chem. Soc.* **2007**, *129*, 14746-14751.
4. Schwieters, C. D.; Kuszewski, J. J.; Tjandra, N.; Clore, G. M. *J. Magn. Res.* **2003**, *160*, 66-74.
5. Phillips, J.C.; Braun, R.; Wang, W.; Gumbart, J.; Tajkhorshid, E.; Villa, E.; Chipot, C.; Skeel, R.D.; Kalé, L.; Schulten, K. *J. Comput. Chem.* **2005**, *26*, 1781.
6. Humphrey, W.; Dalke, A.; Schulten, K. *J. Mol. Graphics* **1996**, *14*, 33.
7. Krimm, S.; Bandekar, J. *Adv. Protein Chem.* **1986**, *38*, 181.
8. Torii, H.; Tasumi, M. *J. Chem. Phys.* **1992**, *96*, 3379.
9. Hamm, P.; Lim, M.; Hochstrasser, R. M. *J. Phys. Chem. B* **1998**, *102*, 6123.
10. Woutersen, S.; Hamm, P. *J. Phys.: Condens. Matter* **2002**, *14*, R1035.
11. Chung, H.S.; Tokmakoff, A. *J. Phys Chem. B* **2006**, *110*, 2888-2898.
12. Ganim, Z.; Tokmakoff, A. *Biophys. J.* **2006**, *91*, 2636-2646.